Complex anion inclusion compounds: Flexible anion-exchange materials

Edward R. Williams and Mark T. Weller*

Department of Chemistry, University of Bath, Claverton Down, Bath, BA2 7AY, UK; Tel:+44 (0) 1225 386531; E-mail:m.t.weller@bath.ac.uk

Rebecca M. Leithall, Robert Raja

School of Chemistry, University of Southampton, Southampton, SO17 1BJ, UK.

Electronic Supplementary Information

Contents

SI-1 Methods and instrumentation
(a) Synthetic methods
(b) Experimental methods and instrumentation
SI-2 Crystallographic information
Table SI-2.1 Crystallographic information
SI-3 Plots describing the relationships between structural features and ionic radii
Figure SI-3.1 Plot showing the linear relationship between lattice parameters and A^+ ionic radius
Figure SI-3.2 Plot showing the linear relationship between the offset angle of the pyrophosphate groups and A^+ ionic radius
SI-4 Cs^+ environments in for $Cs_7Cu_6Cl(P_2O_7)_4.[P(O,OH)_4]$
Figure SI-4.1 Cesium environment in $Cs_7Cu_6Cl(P_2O_7)_4.[P(O,OH)_4]$ in large pores
SI-5 UV-Vis spectra
Figure SI-5.1 UV-vis spectra for $Cs_7Cu_6Cl(P_2O_7)_4.[P(O,OH)_4]$ (green line), $K_9Cu_6(P_2O_7)_4Cl.[P(O,OH)_4]Cl_2$ (red line), $Cs_{0.86}K_{8.14}Cu_6Cl(P_2O_7)_4.Cl_{1.7}$ (black line) and $Cs_7Cu_6Cl(P_2O_7)_4.[P(O,OH)_4]$ stirred in KBr in EtOH (blue line)
SI-6 Sample SEM and EDAX data
Figure/Table SI-6.1 $K_9Cu_6(P_2O_7)_4Cl.[P(O,OH)_4]Cl_2$
Figure/Table SI-6.2 $Cs_9Cu_6(P_2O_7)_4Cl.[P(O,OH)_4]Cl_2$
Figure/Table SI-6.3 $(NH_4)_9Cu_6(P_2O_7)_4Cl.[CuCl_4]Cl_2$
Figure/Table SI-6.4 $Rb_9Cu_6(P_2O_7)_4Cl.[CuCl_4]Cl_2$
Figure/Table SI-6.5 $Cs_7Cu_6Cl(P_2O_7)_4.[P(O,OH)_4]$
Figure/Table SI-6.6 $Rb_9Cu_6(P_2O_7)_4Cl.[PdCl_4]Cl_2$
Figure/Table SI-6.7 $K_9Cu_6(P_2O_7)_4Cl.[PtBr_4]Cl_2$
Figure/Table SI-6.8 $(NH_4)_9Cu_6(P_2O_7)_4Cl.[AuCl_4]Cl_2$
Figure/Table SI-6.9 $K_9Cu_6(P_2O_7)_4Cl.[AuCl_4]Cl_2$
Figure/Table SI-6.10 $Rb_9Cu_6(P_2O_7)_4Cl.[AuCl_4]Cl_2$
Figure SI-6.11 $Rb_9Cu_6(P_2O_7)_4Cl.[AuCl_4]Cl_2$ calcined at 500°C
SI-7 Differences in Cu environments between $Cs_7Cu_6Cl(P_2O_7)_4.[P(O,OH)_4]$ and $Cs_9Cu_6Cl(P_2O_7)_4.[P(O,OH)_4]Cl_2$
Figure SI-7.1 Differenct cross-linking copper environment in $Cs_7Cu_6Cl(P_2O_7)_4.[P(O,OH)_4]$ (left) and in $Cs_9Cu_6Cl(P_2O_7)_4.[P(O,OH)_4]Cl_2$ (right)
Table SI-7.1 Summary of copper coordination environments in four selected compounds
SI-8 Variable temperature studies
Figure SI-8.1 Variable temperature X-ray diffraction data for for $Rb_9Cu_6(P_2O_7)_4Cl.[AuCl_4]Cl_2$
Figure SI-8.2 Thermogravimetric analysis of $Rb_9Cu_6(P_2O_7)_4Cl.[CuCl_4]Cl_2$ and $(NH_4)_9Cu_6(P_2O_7)_4Cl.[CuCl_4]Cl_2$ in air
Figure SI-8.3 Thermogravimetric analysis of $Rb_9Cu_6(P_2O_7)_4Cl.[AuCl_4]Cl_2$ and $K_9Cu_6(P_2O_7)_4Cl.[PtBr_4]Cl_2$ in air

SI-1 Methods and instrumentation

(a) Synthetic methods

All materials used were purchased from Sigma-Aldrich and used without further purification.

(1-2) $A_9Cu_6(P_2O_7)_4Cl_3([P(O,OH,F)_4]/[CuCl_4])$: Copper(II) fluoride (0.0584 g, 0.575 mmol), 85% w.t. orthophosphoric acid (0.1 mL, 1.456 mmol), 50% w.t. AOH (A=Cs 0.2 mL, 1.177 mmol; A=Rb 0.14 mL, 1.191 mmol; A=K 0.1 mL, 1.165 mmol) or 35% NH_3 (0.03 mL, 1.191 mmol) and ACl (A=Cs 0.196 g, 1.165 mmol; A=Rb 0.140 g, 1.165 mmol; A=K 0.087 g, 1.165 mmol; A=NH_4 0.062 g, 1.165 mmol) were mixed in the Teflon® liner of a Parr 23 ml hydrothermal vessel. The hydrothermal vessel was sealed and heated to 448 K for 2 days (493 K for Cs analogue). The pure solid product formed as brilliant green cuboid crystals and was isolated by filtration, washed with distilled water and dried at 60°C

(3) $Cs_7Cu_6(P_2O_7)_4Cl[P(O,OH,F)_4]$: Copper(II) fluoride (0.0584 g, 0.575 mmol), 85% w.t. orthophosphoric acid solution (0.1 mL, 1.456 mmol), 50% w.t. CsOH (0.2 mL, 1.177 mmol) and CsCl (0.0196 g, 0.1165 mmol) were mixed in the Teflon® liner of a Parr 23 ml hydrothermal vessel. The hydrothermal vessel was sealed and heated to 493 K for 2 days. The pure solid product formed as blue cuboid crystals and was isolated by filtration, washed with distilled water and dried at 60°C.

(4-7) $A_9Cu_6(P_2O_7)_4Cl_3[TY_4]$: As **(1-2)**, with a source of $[TY_4]$ added. For **(4)** PdO (0.0176 g, 0.144 mmol) or K_2PdCl_4 (0.0469 g, 0.144 mmol), for **(5)** $HPtCl_6$ (0.07 mL, 0.014 mmol) or K_2PtCl_4 (0.0596 g, 0.144 mmol), for **(6)** K_2PtBr_4 (0.0852 g, 0.144 mmol) and **(7)** $HAuCl_4$ (0.0489 g, 0.144 mmol). The solid products formed as green cuboid crystals and was isolated by filtration,

(b) Experimental methods and instrumentation

Single crystals suitable for structural analysis by X-ray diffraction were isolated from the reaction products. For all compounds cell dimensions and intensity data were recorded at 120K, using a Bruker Nonius APEXII (**1**,**3**) or KappaCCD Roper (**2**) area detector diffractometer mounted at the window of a rotating Mo anode (l(Mo-K_α) = 0.71073Å) operating at 50KV, 85mA. The incident beam on the APEXII side was focused using 10cm confocal mirrors, a graphite monochromator was employed on the KappaCCD side. The crystal-to-detector distance was 30mm. φ and ω scans were carried out to fill the asymmetric unit using 2° frames and 10s per frame exposures. Unit cell determination, data collection and processing were carried out using the programs DirAx[1], COLLECT[2] and DENZO[3] and a multi-scan absorption correction was applied using SADABS[4]. The structures were solved via direct methods[REF] and refined by full matrix least squares[5] on F^2.

Powder X-ray diffraction patterns were obtained by grinding the sample to a fine powder in an agatepestle and mortar and collecting the data on a Siemens D5000 operating with Cu $K_{\alpha 1}$ radiation. Variable temperature powder X-ray diffraction patterns were collected on a Bruker D8 operating with Cu $K_{\alpha 1}$ radiation.

Thermal analysis data were collected using a Stanton-Redcroft simultaneous DTA/TGA STA 1500 systems. SEM micrographs and EDX analysis data were obtained mainly using a Jeol JSM-5910 electron microscope. Additional EDX measurements were performed using a FEI XL30 ESEM.

SI-2 Crystallographic information

Table SI-2.1 Crystallographic information

Structure number	**Product**	**Crystallographic Structure** Lattice type, lattice parameters (Å) and (°) and cell volume (Å^3)	**Refinement details** Space group, *R*-indices and goodness of fit	**Structural features**
(1)	$A_9Cu_6(P_2O_7)_4Cl.[P(O,OH)_4]Cl_2$	Tetragonal; A = K, a=17.4776(4) c=13.3510(4) V=4078.28(2)*	I4/mcm $R1_{all}$=0.084, $wR2_{all}$=0.196 $R1_{obs}$=0.069, $wR2_{obs}$=0.182 GOOF=1.100	Parent structure with disordered free phosphate groups lying along the centre of the channels.
		A= Cs, a=18.0964(2) c=13.6666(2) V=4475.53(1)	I4/mcm $R1_{all}$=0.042, $wR2_{all}$=0.107 $R1_{obs}$=0.039, $wR2_{obs}$=0.104 GOOF=0.749	
(2)	$A_9Cu_6(P_2O_7)_4Cl.[CuCl_4]Cl_2$	Tetragonal; A = [NH$_4$], a=17.8026(3) c=13.5623(3) V=4298.33(1)	I4cm $R1_{all}$=0.079, $wR2_{all}$=0.185 $R1_{obs}$=0.060, $wR2_{obs}$=0.167 GOOF=1.054	As above, with $CuCl_4$ replacing phosphate groups along the centre of the channels.
		A= Rb, a=17.8432(2) c=13.4932(3) V=4295.96(1)	I4cm $R1_{all}$=0.049, $wR2_{all}$=0.120 $R1_{obs}$=0.040, $wR2_{obs}$=0.108 GOOF=0.687	
(3)	$Cs_7Cu_6(P_2O_7)_4Cl.[P(O,OH)_4]$	Orthorhombic; a=16.7592(5) b=18.8341(4) c=13.4990(4) V=4260.88(2)*	Ibam $R1_{all}$=0.088, $wR2_{all}$=0.166 $R1_{obs}$=0.068, $wR2_{obs}$=0.155 GOOF=1.165	Similar structure to **(1)**, however channels are elongated along the *b*-axis.
(4)	$[A_9Cu_6(P_2O_7)_4Cl].[PdCl_4]Cl_2$	Tetragonal; A = K, a=17.5838(5) c=13.3127(9) V=4116.15(3)	I4/mcm $R1_{all}$=0.140, $wR2_{all}$=0.316 $R1_{obs}$=0.116, $wR2_{obs}$=0.300 GOOF=1.201	Same structure as **(2)**, with $CuCl_4$ replaced by TY_4 square planar species.
		A= Rb, a=17.8221(3) c=13.4632(3) V=4276.28(1)	I4/mcm $R1_{all}$=0.042, $wR2_{all}$=0.073 $R1_{obs}$=0.032, $wR2_{obs}$=0.068 GOOF=1.057	
(5)	$[A_9Cu_6(P_2O_7)_4Cl].[PtCl_4]Cl_2$	Tetragonal; A=K a=17.5582(8) c=13.3199 (9) V=4105.46 (4)	I4-c2 $R1_{all}$=0.067, $wR2_{all}$=*0.191* $R1_{obs}$=0.063, $wR2_{obs}$=0.188 GOOF=0.549	
		A=Rb a=17.8054(5) c=13.4697(5) V=4270.33(2)	I4/mcm $R1_{all}$=0.122, $wR2_{all}$=0.154 $R1_{obs}$=0.075, $wR2_{obs}$=0.134 GOOF=1.103	
(6)	$[K_9Cu_6(P_2O_7)_4Cl].[PtBr_4]Cl_2$	Tetragonal; a=17.6178(3) c=13.3285(3) V=4136.99(1)	I4cm $R1_{all}$=0.094, $wR2_{all}$=0.212 $R1_{obs}$=0.068, $wR2_{obs}$=0.188 GOOF=0.866	
(7)	$[A_9Cu_6(P_2O_7)_4Cl].[AuCl_4]Cl_3$	Tetragonal; A = [NH$_4$], a=17.8641(4) c=13.5355(4) V=4319.53(2)	I4/mcm $R1_{all}$=0.135, $wR2_{all}$=0.262 $R1_{obs}$=0.101, $wR2_{obs}$=0.237 GOOF=1.095	
		A = K, a=17.6499(4) c=13.3030(5) V=4144.14(2)	I4cm $R1_{all}$=0.153, $wR2_{all}$=0.335 $R1_{obs}$=0.106, $wR2_{obs}$=0.281 GOOF=0.928	
		A= Rb, a=17.8742(4) c=13.4799(5) V=4306.65(2)*	I4/mcm $R1_{all}$=0.126, $wR2_{all}$=0.147 $R1_{obs}$=0.081, $wR2_{obs}$=0.131 GOOF=1.174	
(7,Rb**)** heated at 500°C for 2 hours	$[Rb_9Cu_6(P_2O_7)_4Cl].[Au(0,III)_{0.55}Cl_{3.18}]Cl_2$	Tetragonal; a=17.7697(17) c=13.4554(10) V=4248.71(7)*	I4/mcm $R1_{all}$=0.051, $wR2_{all}$=0.146 $R1_{obs}$=0.044, $wR2_{obs}$=0.139 GOOF=0.648	Loss of electron density confirms the reduction of $AuCl_4$ species and the ejection of gold metal.

SI-3 Plots describing the relationships between structural features and ionic radii

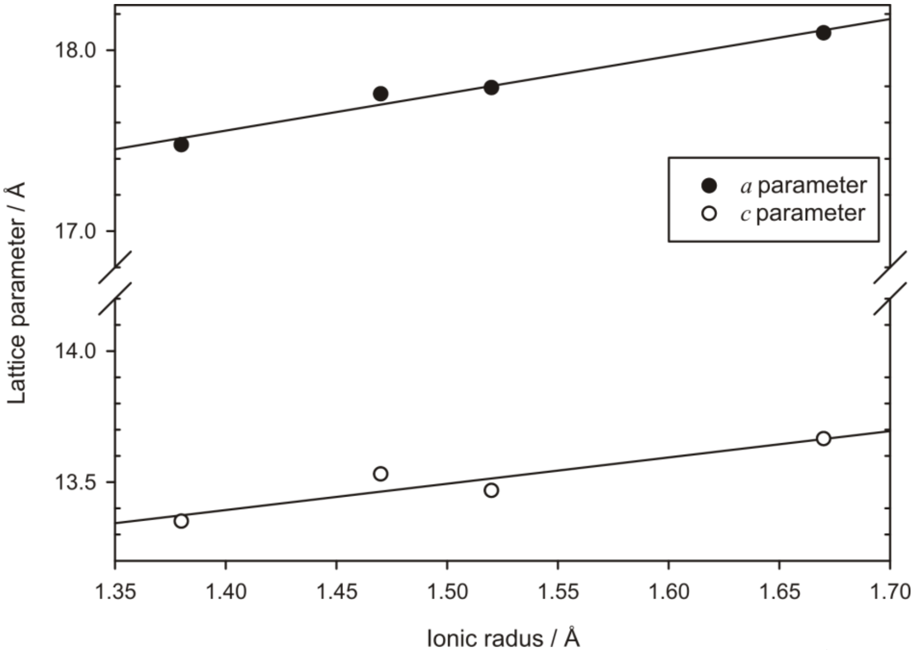

Figure SI-3.1 Plot showing the linear relationship between lattice parameters and A$^+$ ionic radius

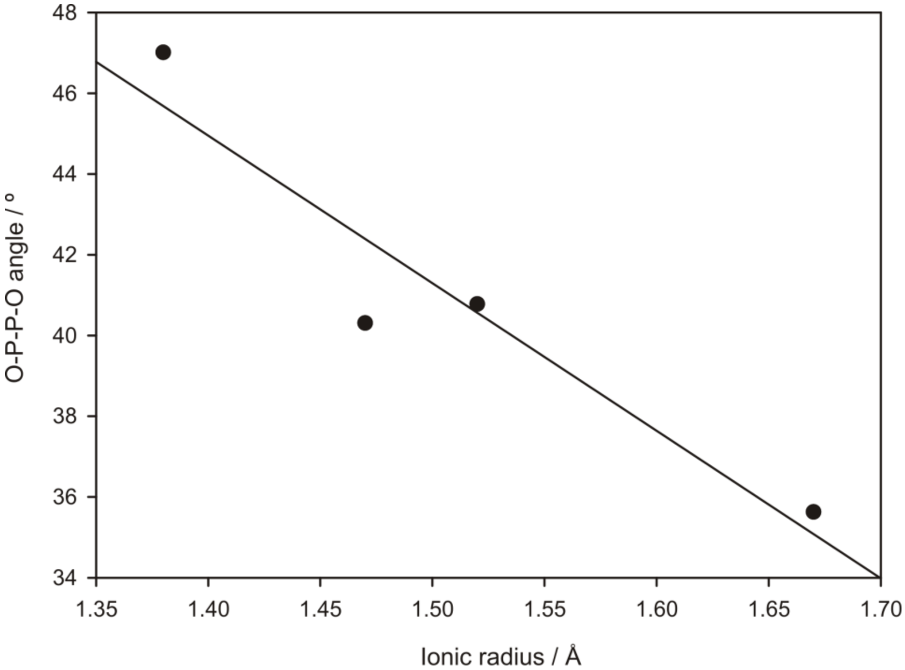

Figure SI-3.2 Plot showing the linear relationship between the offset angle of the pyrophosphate groups and A$^+$ ionic radius

SI-4 Cs^+ environments in for $Cs_7Cu_6Cl(P_2O_7)_4.[P(O,OH)_4]$

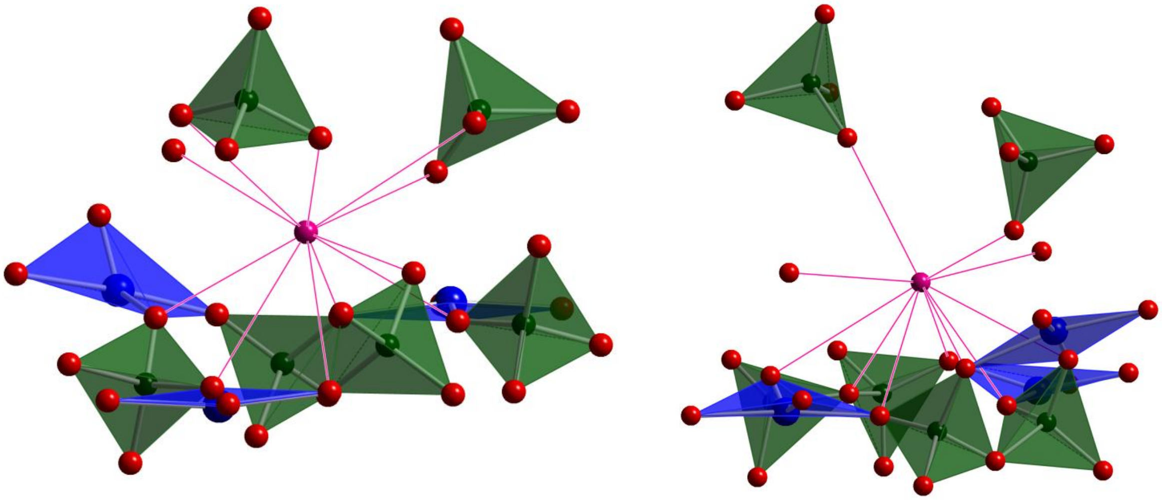

Figure SI-4.1 Cesium environment in $Cs_7Cu_6Cl(P_2O_7)_4.[P(O,OH)_4]$ in large pores (left: Cs2, right: Cs3). Both Cs are 11-coordinate, including interactions with the free phosphates within the channels

SI-5 UV-Vis spectra

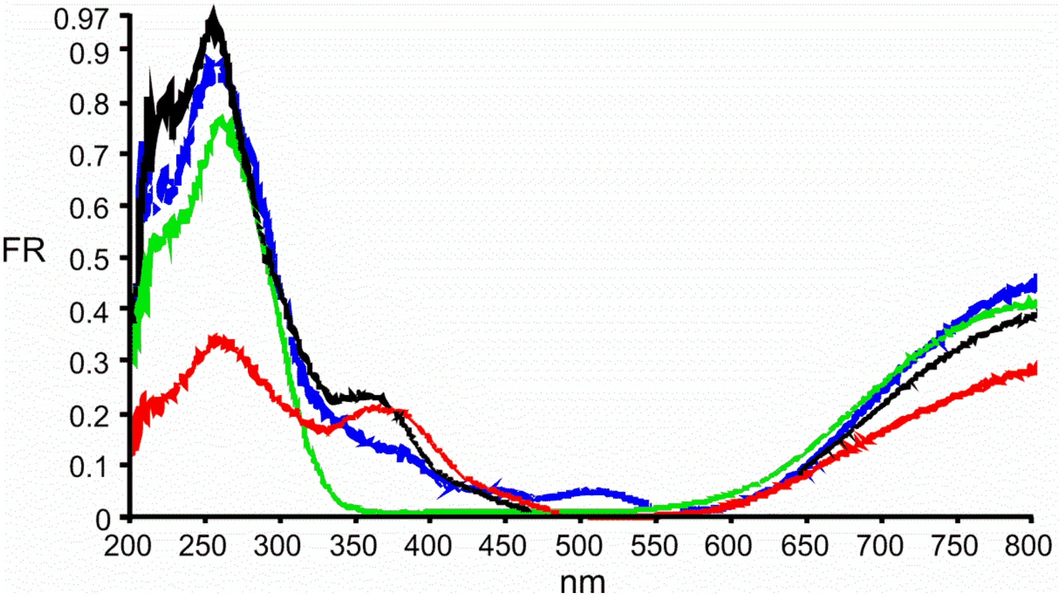

Figure SI-5.1 UV-vis spectra for $Cs_7Cu_6Cl(P_2O_7)_4.[P(O,OH)_4]$ (green line), $K_9Cu_6(P_2O_7)_4Cl.[P(O,OH)_4]Cl_2$ (red line), $Cs_{0.86}K_{8.14}Cu_6Cl(P_2O_7)_4.Cl_{1.7}$ (black line) and $Cs_7Cu_6Cl(P_2O_7)_4.[P(O,OH)_4]$ stirred in KBr in EtOH (blue line).

SI-6 Sample SEM and EDAX data

Collected on Jeol JSM-5910 electron microscope

Figure/Table SI-6.1 $K_9Cu_6(P_2O_7)_4Cl.[P(O,OH)_4]Cl_2$

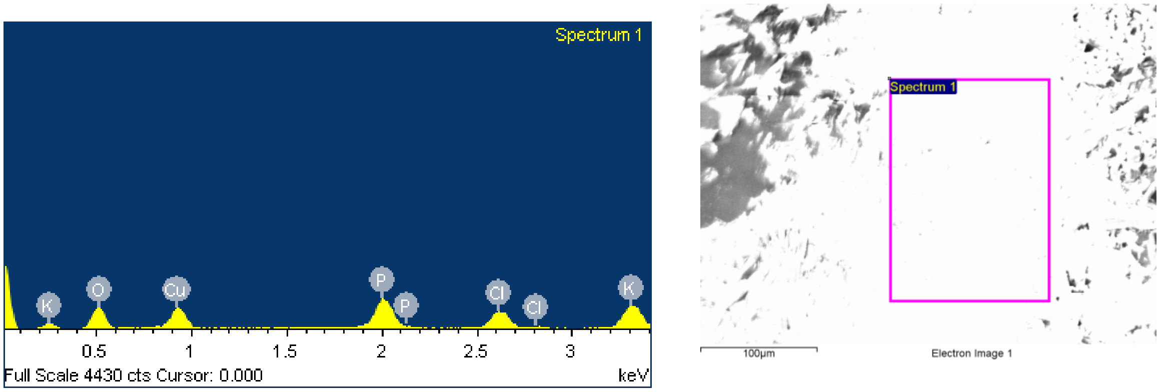

Elements	Theoretical Atomic Ratio	Experimental Atomic %	Experimental Atomic Ratio
K	9	21.14	9
Cu	6	9.43	4
P	9	16.18	7
Cl	3	11.89	5

Figure/Table SI-6.2 $Cs_9Cu_6(P_2O_7)_4Cl.[P(O,OH)_4]Cl_2$

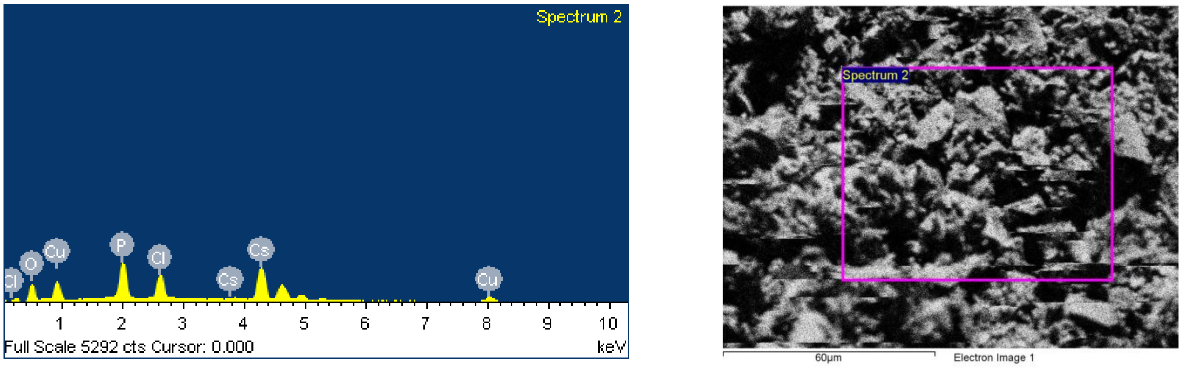

Elements	Theoretical Atomic Ratio	Experimental Atomic %	Experimental Atomic Ratio
Cs	9	25.82	8
Cu	6	20.70	6
P	9	18.65	6
Cl	3	12.84	4

Figure/Table SI-6.3 $[(NH_4)_9Cu_6(P_2O_7)_4Cl].[CuCl_4]Cl_2$

Elements	Theoretical Atomic Ratio	Experimental Atomic %	Experimental Atomic Ratio
Cu	7	22.48	6
P	8	23.87	6
Cl	7	22.47	6

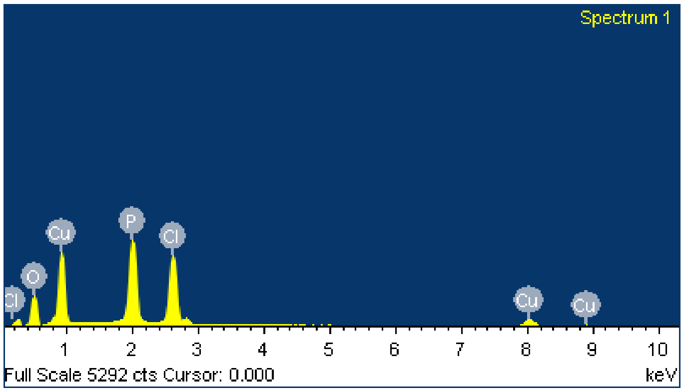

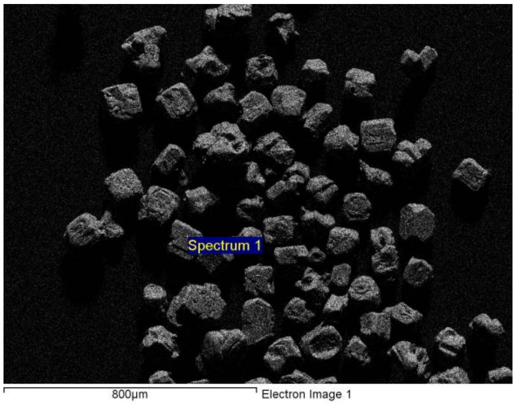

Figure/Table SI-6.4 $Rb_9Cu_6(P_2O_7)_4Cl.[CuCl_4]Cl_2$ *

Elements	Theoretical Atomic Ratio	Experimental Atomic %	Experimental Atomic Ratio
Rb	9	21.47	7
Cu	7	8.90	3
P	8	20.77	7
Cl	7	10.52	3

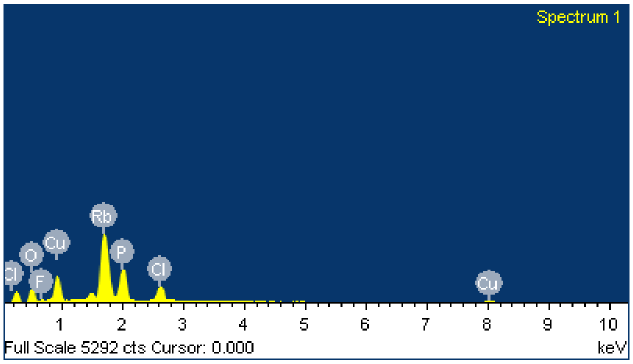

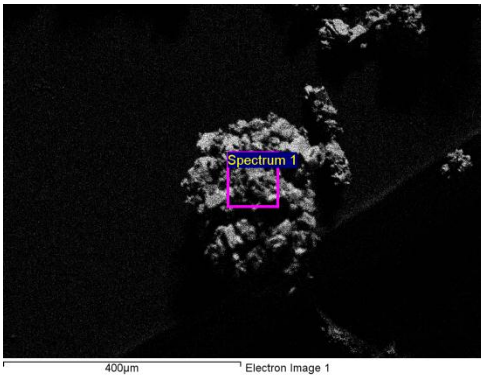

Figure/Table SI-6.5 $Cs_7Cu_6Cl(P_2O_7)_4.[P(O,OH)_4]$

Elements	Theoretical Atomic Ratio	Experimental Atomic %	Experimental Atomic Ratio
Cs	7	15.49	9
Cu	6	9.17	6
P	9	18.01	10
Cl	1	1.68	1

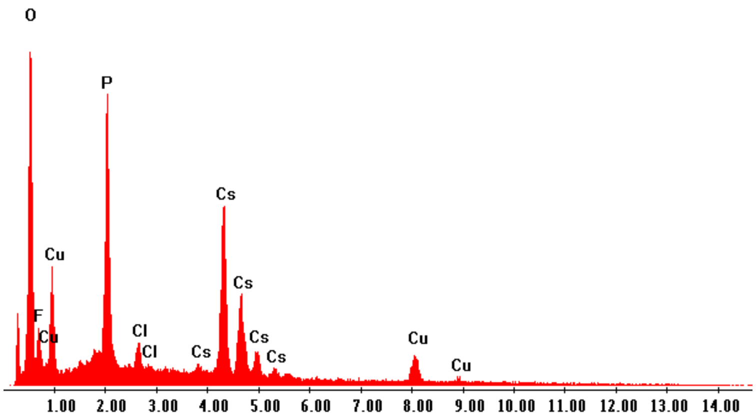

Figure/Table SI-6.6 $Rb_9Cu_6(P_2O_7)_4Cl.[PdCl_4]Cl_2$ *

Elements	Theoretical Atomic Ratio	Experimental Atomic %	Experimental Atomic Ratio
Rb	9	12.09	3
Cu	6	11.67	3
P	8	31.64	8
Cl	7	12.40	12
Pd	1	4.02	1

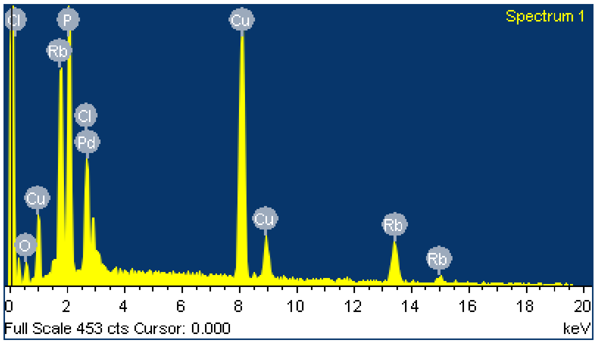

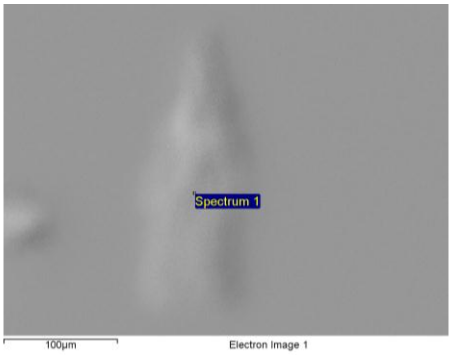

Figure/Table SI-6.7 $K_9Cu_6(P_2O_7)_4Cl.[PtBr_4]Cl_2$

Elements	Theoretical Atomic Ratio	Experimental Atomic %	Experimental Atomic Ratio
K	9	19.20	10
Cu	6	8.43	4.5
P	8	15.50	8
Cl	3	7.94	4
Pt	1	1.88	1
Br	4	6.43	3.5

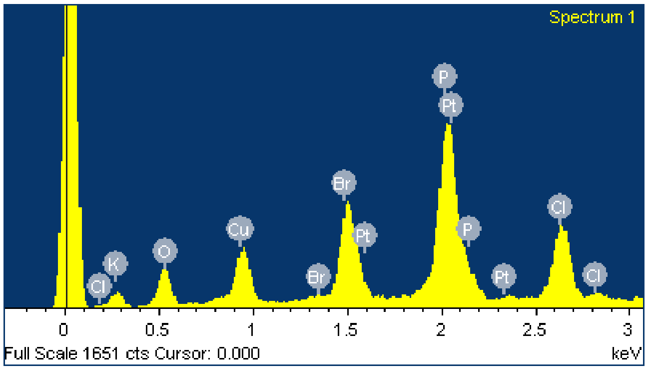

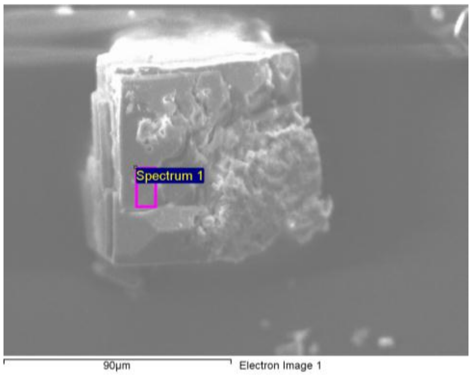

Figure/Table SI-6.8 $(NH_4)_9Cu_6(P_2O_7)_4Cl.[AuCl_4]Cl_2$ *

Elements	Theoretical Atomic Ratio	Experimental Atomic %	Experimental Atomic Ratio
Cu	6	14.25	16.5
P	8	14.22	16.5
Cl	7	10.38	12
Au	1	0.86	1

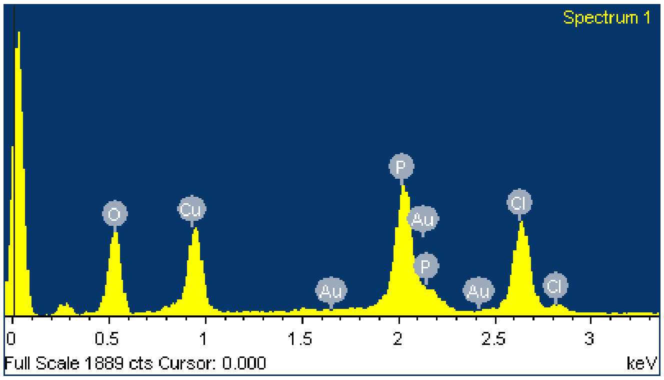

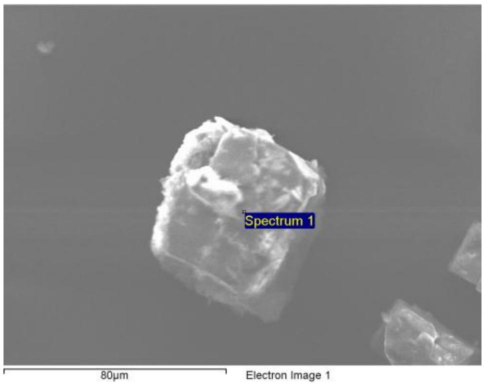

Figure/Table SI-6.9 $K_9Cu_6(P_2O_7)_4Cl.[AuCl_4]Cl_2$

Elements	Theoretical Atomic Ratio	Experimental Atomic %	Experimental Atomic Ratio
K	9	17.06	9
Cu	6	10.19	5
P	8	14.19	7
Cl	7	16.07	8
Au	1	1.93	1

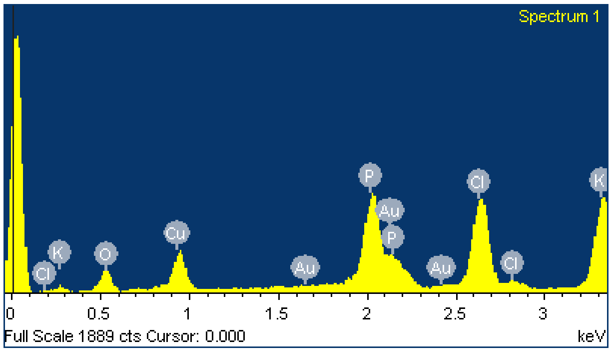

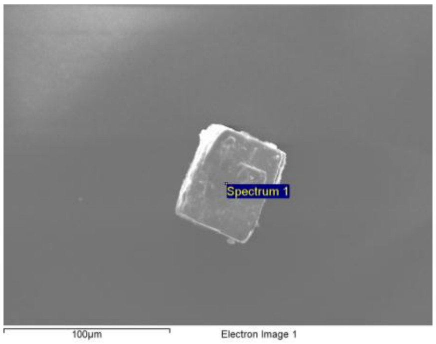

Figure/Table SI-6.10 $Rb_9Cu_6(P_2O_7)_4Cl.[AuCl_4]Cl_2$

Elements	Theoretical Atomic Ratio	Experimental Atomic %	Experimental Atomic Ratio
Rb	9	14.12	5.5
Cu	6	11.04	4
P	8	13.84	7
Cl	7	14.30	5.6
Au	1	2.57	1

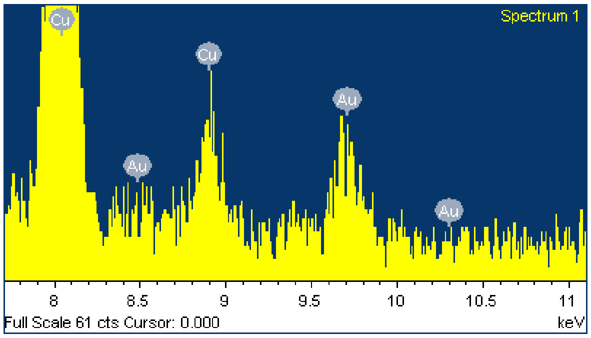

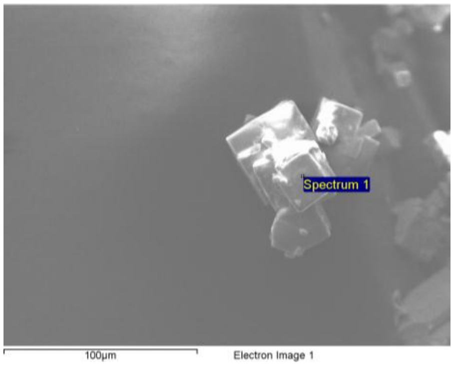

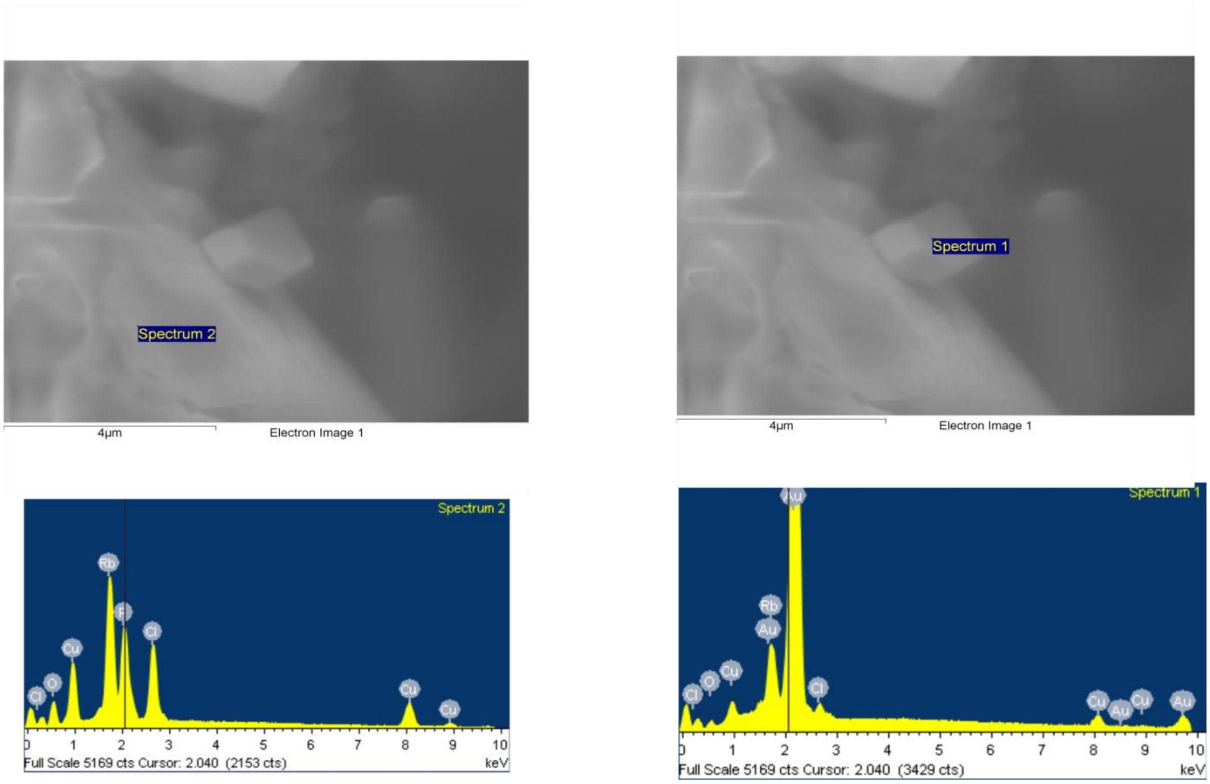

Figure SI-6.11 $Rb_9Cu_6(P_2O_7)_4Cl.[AuCl_4]Cl_2$ calcined at 500°C

*****Samples found to be unpure, resulting in inconsistencies between theoretically atomic ratios and those found experimentally.

SI-7 Differences in Cu environments between $Cs_7Cu_6Cl(P_2O_7)_4.[P(O,OH)_4]$ and $Cs_9Cu_6Cl(P_2O_7)_4.[P(O,OH)_4]Cl_2$

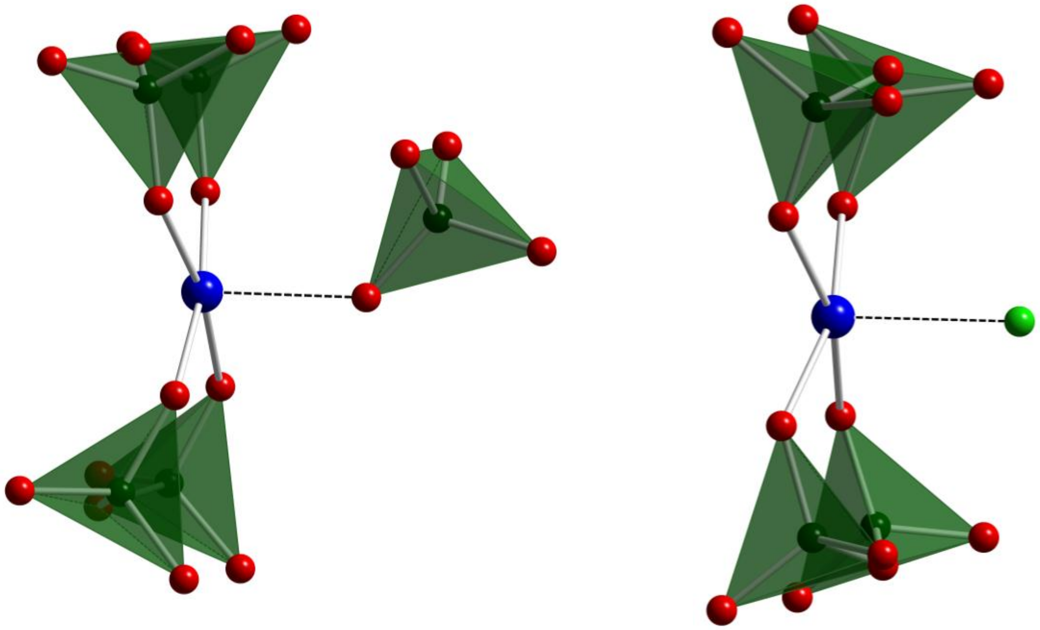

Figure SI-7.1Differenct cross-linking copper environment in $Cs_7Cu_6Cl(P_2O_7)_4.[P(O,OH)_4]$ (left) and in $Cs_9Cu_6Cl(P_2O_7)_4.[P(O,OH)_4]Cl_2$ (right)

Table SI-7.1 Summary of copper coordination environments in four selected compounds

Compound	Color	Cross-linking copper environment	Bond distances (Å)
$K_9Cu_6(P_2O_7)_4Cl.[P(O,OH)_4]Cl_2$	Bright lime green	CuO_4Cl	Cu-O 1.933(5) Cu-Cl 2.715(3)
$Rb_9Cu_6(P_2O_7)_4Cl.[CuCl_4]Cl_2$	Gold/green	CuO_4Cl	Cu-O 1.954(4) Cu-Cl 2.634(3)
$Cs_9Cu_6Cl(P_2O_7)_4.[P(O,OH)_4]Cl_2$	Bright lime green	CuO_4Cl	Cu-O 1.967(6) Cu-Cl 2.533(3)
$Cs_7Cu_6(P_2O_7)_4Cl.[P(O,OH)_4]$	Pale blue	$CuO_4(O)$	Cu-O 1.931(9), 1.941(9) Cu-(O) 2.281(16)

SI-8 Variable temperature studies

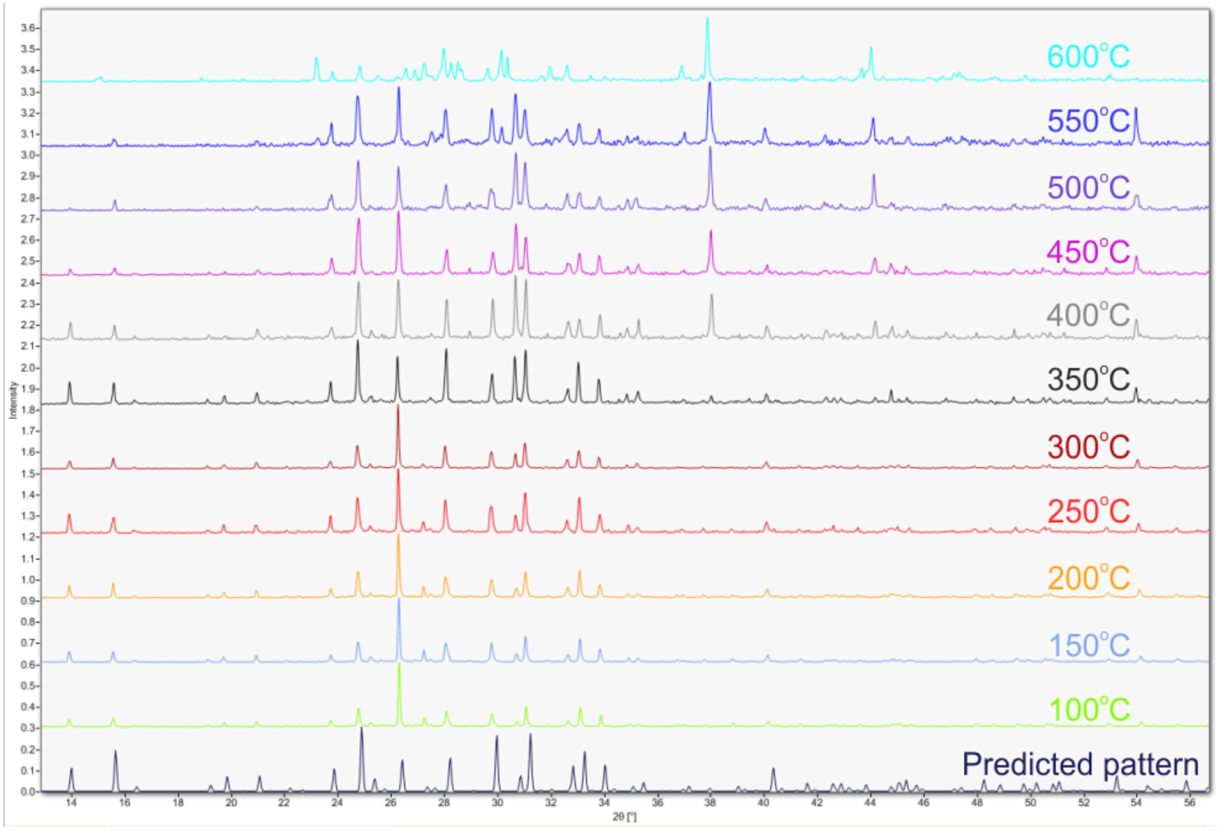

Figure SI-8.1 Variable temperature X-ray diffraction data for $Rb_9Cu_6(P_2O_7)_4Cl.[AuCl_4]Cl_2$. Top pattern displays predicted pattern, subsequent patterns were collected at 50 °C intervals between 100 and 600 °C.

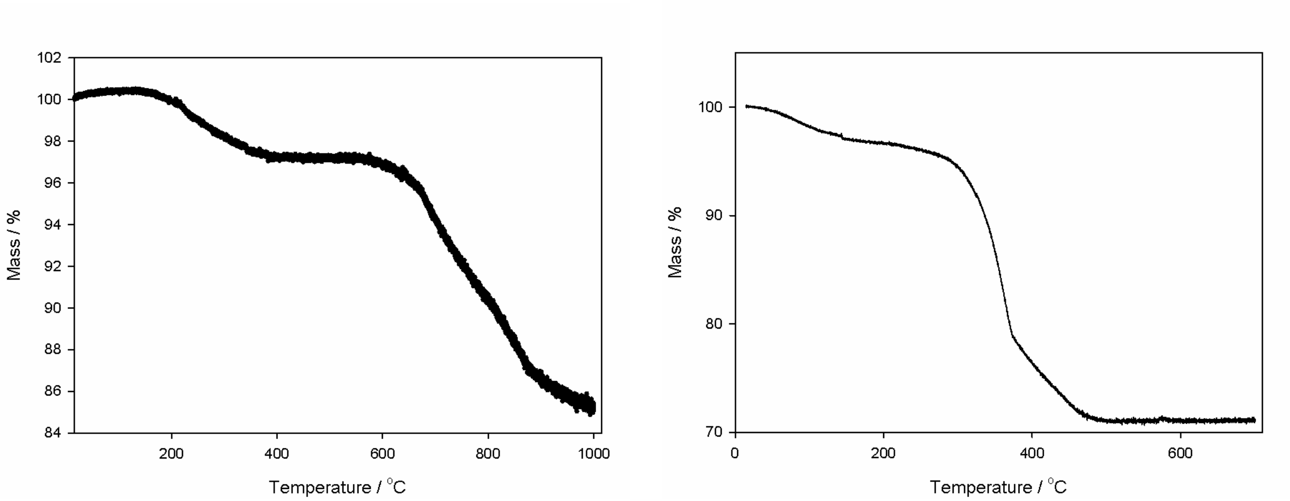

Figure SI-8.2 Thermogravimetric analysis of $Rb_9Cu_6(P_2O_7)_4Cl.[CuCl_4]Cl_2$ and $(NH_4)_9Cu_6(P_2O_7)_4Cl.[CuCl_4]Cl_2$ in air

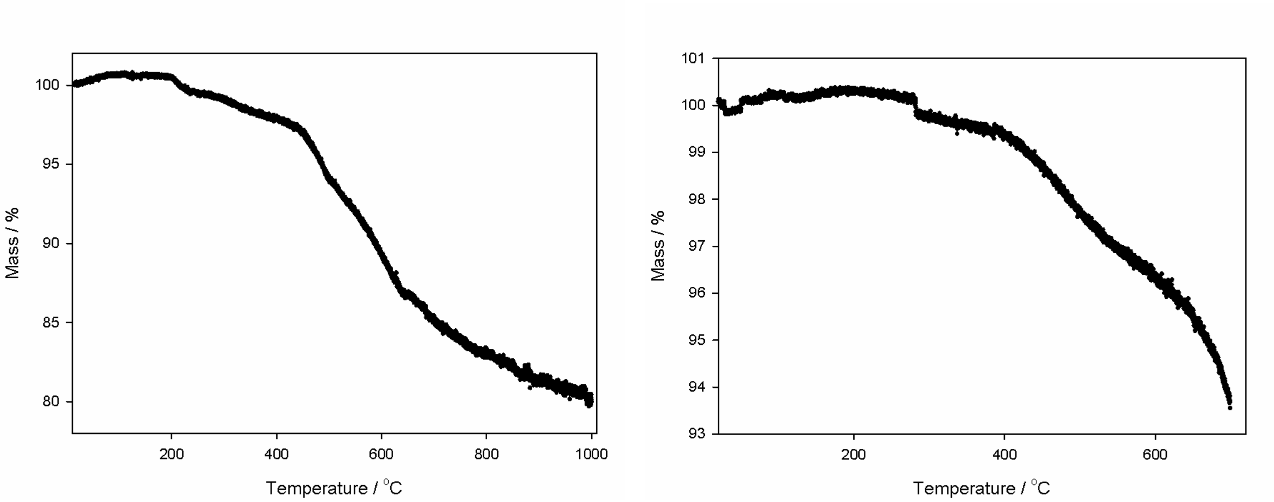

Figure SI-8.3 Thermogravimetric analysis of $Rb_9Cu_6(P_2O_7)_4Cl.[AuCl_4]Cl_2$ and $K_9Cu_6(P_2O_7)_4Cl.[PtBr_4]Cl_2$ in air

References

1 Duisenberg, A. J. M. Indexing in single-crystal diffractometry with an obstinate list of reflections. *Journal of Applied Crystallography* **25**, 92-96, doi:10.1107/s0021889891010634 (1992).
2 Nonius, B. V. *COLLECT data collection software*. (1998).
3 Otwinowski, Z. & Minor, W. Processing of X-ray diffraction data collected in oscillation mode. *Macromolecular Crystallography, Pt A* **276**, 307-326, doi:10.1016/s0076-6879(97)76066-x (1997).
4 Sheldrick, G. M. *SADABS - Bruker Nonius area detector scaling absorption correction - V2.10*.
5 Sheldrick, G. M. *Release 97-2*. (University of Göttingen, Germany, 1997).